Observing the Transition from Stark-Shifted, Strong-Field Resonance to Nonadiabatic Excitation†

Stanley M. Smith,[‡,||] Dmitri A. Romanov,[§,||] George Heck,[§,||] H. Bernhard Schlegel,[⊥] and Robert J. Levis*,[‡,||]

Department of Chemistry, Department of Physics, and Center for Advanced Photonics Research, Temple University, Philadelphia, Pennsylvania 19122, and Department of Chemistry, Wayne State University, Detroit, Michigan 48202

Received: July 31, 2009; Revised Manuscript Received: November 3, 2009

Time-dependent Hartree−Fock simulations for a linear triatomic molecular monocation (CO_2^+) interacting with a 5 fs, 800 nm, strong field laser pulse were performed to explore the excitation mechanisms in a molecular cation. Fourier analysis of the time-dependent residual dipole moment reveal a nonmonotonic behavior in the amplitude of the 5.18 eV feature in the excitation spectra of the molecular monocation with increasing intensity, suggesting a change in the excitation mechanism. Calculations performed for different carrier frequencies of the laser field reveal that the mechanism changes from resonant multiphoton excitation to nonadiabatic excitation. In the resonant multiphoton excitation regime, a slight variation of the laser pulse duration (fwhm) reveals a nonlinear increase in the peak height of the multiphoton resonant state, and Stark-shifting of the multiphoton resonant state is observed for an increase in intensity. Nonadiabatic excitation from TDHF compares well with the analytical theory for nonadiabatic excitation.

Introduction

The goal of coherent quantum control is to guide a system to a desired product state through interaction with a tailored laser pulse at the expense of all other possible product states.[1−11] Often, this is accomplished in the strong-field regime where the electric field is on the order of the molecular electric field binding the valence electrons. The interaction of a strong, nonresonant laser field with a molecule is governed by the coupling of the laser field with the molecular electrons in the system.[12−15] All nonresonant interactions can be classified as adiabatic (when the molecular energy states follow the field without interstate electronic transitions) or nonadiabatic (when interstate electronic transitions occur and result in energy deposition from the field to the molecule). Adiabatic nonresonant interactions can result in single[16−18] or multiple[19,20] ionization events. This process is described by quasistatic theories of tunnel ionization.[17,21] A single ionization event usually leads to formation of a intact molecular ion,[16,18] possibly in the ground electronic state. Multiple ionization can result in energetic dissociation of the molecules in a process known as Coulomb explosion.[22,23] Nonadiabatic laser−molecule interactions can also result in outcomes such as nonresonant electronic excitation,[24] fragmentation to neutral products,[25,26] ionization, dissociative ionization,[27,28] and nuclear rearrangement.[2]

Strong laser fields not only produce nonresonant interactions, but they can also produce resonant interactions due to dynamic Stark-shifting[7−9,29,30] in atoms and molecules. This Stark-shifting can induce temporary multiphoton resonances between excited states in the atom or molecule (similar to Freeman[31] resonances in above threshold ionization spectra). The high density of electronic states in a molecule implies the possibility of considerable Stark-shifting in the vicinity of a multiphoton resonance. Such resonances play an important role in molecular excitation. The duration of the resonant interaction explicitly determines the extent of excitation for that particular state in the molecule. For an ultrashort, strong-field laser pulse, the resonance is normally transient and will have only a limited impact on the total excitation spectrum. In particular, when the laser pulse is on the order of 3 cycles of the optical field, all possible resonances are expected to be transient, and significant resonant excitation can occur only when the optimal Stark-shifting occurs at or near the peak of the pulse envelope. At this point, the field envelope changes slowly, maintaining the resonance condition for a longer period.

Laser pulses on the order of a few cycles of the optical field generally couple only to the electronic degrees of freedom in a molecule or molecular ion because there is no time for nuclear motion to occur during the pulse.[32] (The hydrogen molecule is an important and well-studied exception.) After the laser field has returned to zero, the molecule may remain in a superposition of excited states that can continue to evolve. This evolution typically includes nuclear dynamics that may lead to bond-breaking and bond-formation.[2] For such ultrashort, strong-field laser pulses, excitation, ionization, and rescattering processes are the main processes induced by the electric field. When laser pulses are long compared to the period of characteristic vibrational frequencies of a molecule, resonant electron excitation and nuclear motion can occur during the pulse. This nuclear motion not only determines bond breaking and bond formation; it has also been shown to enhance ionization.[33]

We are concerned here with the approximate bound state electron dynamics of a linear triatomic molecular monocation, CO_2^+. The focus is in determining the conditions for inducing resonant or nonadiabatic mechanisms during the excitation process or, equivalently, which process dominates the excitation for a given set of laser pulse parameters, such as intensity or

† Part of the "Barbara J. Garrison Festschrift".
* Corresponding author. E-mail: rjlevis@temple.edu.
‡ Department of Chemistry, Temple University.
§ Department of Physics, Temple University.
|| Center for Advanced Photonics Research, Temple University.
⊥ Wayne State University.

10.1021/jp907372k
Published on Web 12/30/2009

laser carrier frequency. Ultimately, our goal is to describe the characteristic differences in the excitation spectra that define the type of excitation mechanism dominating the laser-molecule interaction when an ultrashort, 3-cycle pulse interacts with our approximation of CO_2^+.

Here, we incorporate nonadiabatic and multielectron effects into the theoretical description of the strong-field excitation of CO_2^+. We consider the model situation wherein the short pulse interacts with the ion that is initially in its ground electronic state. We use time-dependent Hartree−Fock theory to investigate the interaction of a few-cycle, strong-field laser pulse with the molecule as a first step to analyzing the attosecond bound state electron dynamics. We investigate the bound state excitation profiles by applying a Fourier transform to the residual dipole moment oscillations for a three-cycle Gaussian pulse shape. The intensity dependence reveals both resonant and nonadiabatic excitation. Varying the excitation frequency reveals the Stark shift of the lowest-energy excited state. Finally, we describe the distinct characteristics of strong-field resonant and nonadiabatic excitation.

Method

To investigate the bound state electron dynamics during the interaction of shaped light pulses with molecules, we employ the time-dependent Hartree−Fock (TDHF) equations. In an orthonormal basis, these equations can be written in terms of the Fock matrix, **F**, and the one-electron density matrix, **P**.

$$i\frac{\mathrm{d}\mathbf{P}(t_i)}{\mathrm{d}t} = [\mathbf{F}(t_i), \mathbf{P}(t_i)] \tag{1}$$

The Fock matrix depends not only on the time-dependent electric field, $\mathbf{E}(t)$, but also on the time-dependent density matrix. Efficient integration of this equation has been described previously.[34] The property commonly used to analyze the electron response to the laser field is the instantaneous dipole moment given by

$$\mu(t_i) = \sum Z_A R_A - tr(\boldsymbol{D'P'}(t_i)) \tag{2}$$

where Z_A is the charge on atom A, R_A is the distance of atom A from the center of the coordinate system, $\mathbf{D'}$ is the dipole moment integrals in the atomic orbital (AO) basis, and $\mathbf{P'}$ is the density matrix in the AO basis.

To simulate the response of the electrons to a short laser pulse, a Gaussian envelope shape was used to modulate the electric, which is defined by

$$\mathbf{E}(t) = E_{\max} \exp\left(\frac{-t^2}{2\alpha^2}\right) \sin(\omega t + \phi) \tag{3}$$

where α is related to the full width at half-maximum (fwhm) (fwhm $= 2\alpha(2 \ln 2)$, ω is the laser frequency, and $E_{\max}$ is the maximum electric field.

Electron dynamics in the field were simulated using the development version of the Gaussian[35] series of programs with the addition of the unitary transform time-dependent Hartree−Fock algorithm (UT-TDHF).[34] Calculations were performed at the HF level of theory using the aug-cc-pVTZ[36,37] basis set for carbon dioxide. At the HF/aug-cc-pVTZ level of theory for the ground state of CO_2, the equilibrium C−O bond distance is 1.1363 Å, which is comparable to the experimentally measured bond length of 1.162 Å.[38] Assuming vertical ionization and that the interaction with the laser pulse occurred before the monocation geometry could relax, the bond distance was kept at the CO_2 equilibrium bond distance for these calculations. The corresponding excited states from time-dependent Hartree−Fock theory with transition dipoles along the molecular axis are listed in Table 1. The integrations were carried out for 24 fs with a step size of 0.0012 fs (0.05 au).

The calculations for CO_2^+ represent an approximation to the electronic response of the bound state electron dynamics in an ion interacting with a short laser pulse at the Hartree−Fock level of theory. This approximation for the bound state ion dynamics does not exactly describe the exact electron dynamics because correlation is not explicitly taken into account. However, the approximation is accurate enough to demonstrate the changes in the excitation spectrum due to resonant multiphoton or nonadiabatic excitation. Ionization from states lying more deeply bound than the HOMO (HOMO − 2, for example) are likely involved in the dynamics and will be explored in a subsequent publication. To determine whether continuum states are accessed during the excitation process, we can calculate the ionization probability. A simple calculation reveals that the ionization probability[39] for CO_2^+ is 0.01 for the largest intensity of 5×10^{14} W/cm^2. This suggests that bound state dynamics dominate the ionic response at the intensities investigated.

The presence of residual dipole moment oscillations after the laser pulse reveals the effects of either resonant or nonresonant excitation in the molecule. The states excited may be revealed by Fourier transforming the residual dipole oscillations.[40,41] The power spectrum obtained reflects the composition of the multielectron excitation in terms of the field-free states. All Fourier transforms of the residual dipole moments were calculated over the interval from 12 to 24 fs. The height of each peak in the Fourier transform will be referred to as the Fourier amplitude or amplitude.

Results and Discussion

We are concerned with resonances and nonadiabatic excitation in a ion exposed to an intense, few-cycle laser pulse near 800 nm. In such a pulse, the envelope changes so rapidly that a large number of excited states in a molecule are considerably Stark-shifted and can be in multiphoton resonance momentarily with the field carrier frequency. Such accidental resonances should be discernible from strictly nonadabatic excitation by analyzing the spectral composition of the residual dipole oscillations as a function of laser intensity and carrier frequency.

Figure 1 shows the response of the residual dipole moment of CO_2^+ to a laser pulse with fwhm = 3.5 fs and a field frequency of 0.06 au, corresponding to a photon energy of 1.63 eV, with the electric field polarized along the molecular axis. Figure 1a displays the Fourier transform of the residual dipole moment oscillations for a Gaussian envelope pulse (described by eq 3) with an intensity $I = 1.3 \times 10^{14}$ W/cm^2. The first peak in Figure 1a can be ascribed to the lowest-lying excited state of CO_2^+ occurring at 5.18 eV at the HF/aug-cc-pVTZ level of theory. At the MRCISD/aug-cc-pVTZ level of theory, this state energy is 5.03 eV, whereas at the CIS/aug-cc-pVTZ level, this state energy is 5.81 eV. Experimental results[42,43] for this state are not directly comparable because state energy, measured from emission spectroscopy, is measured at the ion geometry. This geometry was determined by theoretical[44,45] simulation of the emission spectrum. The second, third, and fourth peaks observed are excited states found at 9.0, 12.5, and 15.4 eV, respectively. The ionization potential at this level of theory is 22.56 eV via Koopman's theorem, so the excitation spectrum shown in Figure 1a describes the approximated bound state dynamics of CO_2^+. For all four excited states, the transition dipole moments with the ground state lie parallel to the molecular axis.

TABLE 1: Excited State Energies and Transition Dipole Moments along the Molecular Axis for CO_2^+ at the HF/aug-cc-pVTZ Level of Theory

main transitions[a] (TDHF coefficient)	energy (eV) from TDHF	oscillator strength	transition dipole moment
HOMO − 1 → SOMO (1.15)	5.18	0.083	0.81
HOMO → LUMO + 1 (0.22)			
HOMO → LUMO + 1 (0.92)	9.03	0.014	0.25
SOMO → LUMO + 2 (0.60)			
HOMO → LUMO + 1 (0.67)	12.49	0.05	0.39
SOMO → LUMO + 2 (0.65)			
HOMO → LUMO + 1 (0.61)	15.44	0.59	1.3
SOMO → LUMO + 2 (0.36)			
HOMO → LUMO + 3 (0.25)			
HOMO − 3 → LUMO (0.24)			
HOMO → LUMO + 3 (0.77)	17.10	0.081	0.44
HOMO − 3 → LUMO (0.44)			
HOMO − 3 → LUMO (0.60)	17.61	0.094	0.47
HOMO → LUMO + 3 (0.46)			
HOMO − 2 → LUMO (0.34)			
SOMO → LUMO + 4 (0.80)	18.58	0.16	0.59
HOMO − 2 → LUMO (0.31)			
SOMO → LUMO + 14 (0.29)			
SOMO → LUMO + 2 (0.28)			
HOMO − 2 → LUMO (0.68)	19.21	0.42	0.062
HOMO − 3 → LUMO (0.34)			
SOMO → LUMO + 4 (0.30)			
HOMO − 3 → LUMO + 9 (0.23)			
HOMO − 1 → LUMO +8 (0.88)	21.66	0.0004	0.029
HOMO → LUMO + 13 (0.39)			
HOMO − 3 → LUMO + 6 (0.49)	22.13	0.019	0.19
HOMO − 4 → LUMO + 4 (0.41)			
HOMO − 3 → LUMO + 16 (0.36)			
SOMO → LUMO + 14 (0.83)	23.13	0.0016	0.053
SOMO → LUMO + 4 (0.29)			
HOMO − 1 → LUMO + 8 (0.24)			
HOMO − 3 → LUMO + 9 (0.68)	23.67	0.10	0.42
HOMO − 4 → LUMO + 14 (0.36)			
HOMO − 3 → LUMO (0.32)			
HOMO → LUMO + 18 (0.52)	24.26	0.018	0.19
HOMO − 2 → LUMO + 7 (0.49)			
HOMO → LUMO + 18 (0.50)	24.48	0.020	0.18
HOMO − 2 → LUMO + 7 (0.40)			
HOMO − 2 → LUMO + 6 (0.39)			
HOMO − 3 → LUMO + 11 (0.97)	24.70	0.00	0.0039

[a] SOMO = singly occupied molecular orbital.

The maximum of the electric field was varied for the Gaussian pulse to explore the effects on the excited state spectra. In this experiment, the carrier frequency, fwhm, and carrier envelope phase were held constant at $\omega = 0.06$ au, 3.5 fs, and $\phi = 0$, respectively. Figure 1b shows the excitation spectra for intensities of 0.875, 1.3, 2, 2.5, 3, 4, and 5×10^{14} W/cm^2. The response of the excitation volume (area under the Fourier transform) increases until a local maximum is attained at an intensity of 1.3×10^{14} W/cm^2, then decreases to a minimum at $I = 2.5 \times 10^{14}$ W/cm^2 before the volume starts increasing again for intensities from 2.5 to 5×10^{14} W/cm^2. The response of the excitation volume observed conflicts with the prediction of nonadiabatic multielectron excitation theory (NME).[12−15] NME theory describes the probability to make a nonresonant transition from the ground state, $|g\rangle$, to some excited state, $|Ex\rangle$, (with the approximation that $\omega \ll \Delta_0$) per laser half-cycle as

$$P_{|g\rangle\rightarrow|Ex\rangle} = \exp\left[\frac{-\pi\Delta_0^2}{4\hbar\omega\varepsilon_0\sqrt{\mu^2 + \frac{\alpha_g^*\Delta_0}{4}}}\right] \quad (4)$$

where Δ_0 is the energy difference between the two states, ω is the laser frequency, ε_0 is the maximum magnitude of the electric field, μ is the transition dipole moment between the two states, and α_g^* is the dynamic polarizability of the ground state with the contribution of the Δ_0 state removed. The most recent version of NME theory[14,15] extends a two-state, single active electron (SAE) model to a multielectron model through inclusion of the dynamic polarizability. The three key steps summarizing this model include (i) nonadiabatic absorption of energy, resulting in an electron gaining ponderomotive energy (defined as $U_p = e^2\varepsilon_o^2/4m_e\omega^2$); (ii) formation of a quasicontinuum in the excited electronic state manifold; and (iii) coupling to a doorway state in the quasicontinuum. The electron ponderomotive energy increases in parallel with the formation of the quasicontinuum. Once the ponderomotive potential is equal to Δ_0, the electron makes the transition to the doorway state and continues to quickly climb through the quasicontinuum, experiencing classical plasmalike energy absorption. This leads to either an excited or an ionized molecule after the laser pulse has passed. As in the case of transition to a true continuum, the total excitation probability is obtained by summation of the conditional probabilities over half-cycles of the laser pulse. By the mth half-cycle of the pulse, the total excitation probability for a neutral molecule is

$$P_{\text{total}}^{\text{neutral}}(m) = 1 - \prod_{n=1}^{m}[1 - P_{|g\rangle\rightarrow|DS\rangle}(n)] \quad (5)$$

where the dependence, $P_{|g\rangle\rightarrow|DS\rangle}(n)$, on the cycle number, n, is determined by the envelope of the laser pulse. NME theory

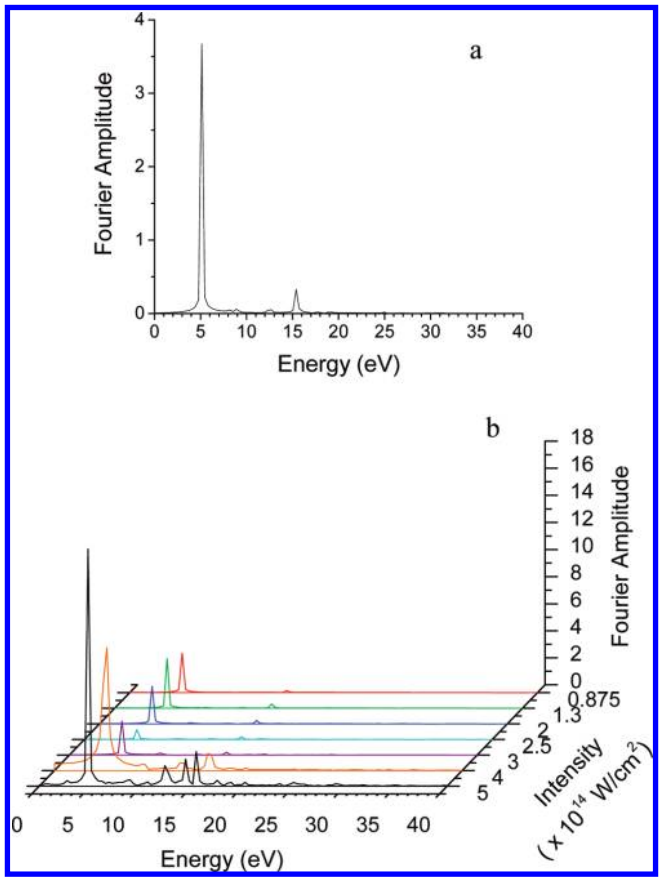

Figure 1. CO_2^+ excited state spectra for a pulse with $I = 1.3 \times 10^{14}$ W/cm^2, fwhm = 3.5 fs, $\omega = 0.06$ au, and a phase of $\phi = 0$ for (a) Gaussian and (b) Gaussian pulse envelope with field intensities of 0.875, 1.3, 2.0, 2.5, 3.0, 4.0, and 5.0×10^{14} W/cm^2.

suggests that a higher-intensity electric field should have a greater excitation probability than a lower intensity electric field and, therefore, does not explain the decrease in Fourier amplitude of the 5.18 eV peak at lower intensities (i.e., 0.875, 1.1, and 2×10^{14} W/cm^2). If nonadiabatic excitation is the dominant excitation mechanism, the additive effect of eq 5 must occur. Thus, the change in the excitation volume for the 5.18 eV feature as a function of laser intensity can not be explained by NME, suggesting that another excitation mechanism is involved.

(a) Resonant Multiphoton Excitation. The 5.18 eV feature is nearly in resonance with a three-photon process and may result from resonant multiphoton excitation (a Freeman resonance).[31] The response of the Fourier amplitude may be explained by the Stark-shifting of the 5.18 eV state into resonance with a multiple of the laser frequency at $\omega = 0.06$ au, corresponding to a photon energy of 1.63 eV. The three-photon process has an energy of 4.89 eV at this frequency. To analyze the effect of this resonance more explicitly, the Fourier amplitude is plotted for seven different field intensities (with field parameters fwhm = 3.5 fs, $\omega = 0.06$ au, and $\phi = 0$) in Figure 2. This Figure reveals a maximum in the Fourier amplitude of the 5.18 eV state at an intensity of 1.1×10^{14} W/cm^2 with a decrease above and below this intensity. Figure 2 also shows that the near-three-photon resonance is relatively broad in intensity from about 0.875 to 2.0×10^{14} W/cm^2, with the three central intensities of 1.1, 1.3, and 1.5×10^{14} W/cm^2 having nearly the same Fourier amplitudes of 3.67, 3.65, and 3.65, respectively.

To explore this near-three-photon resonance in greater detail, the Fourier amplitude of the 5.18 eV state was determined for

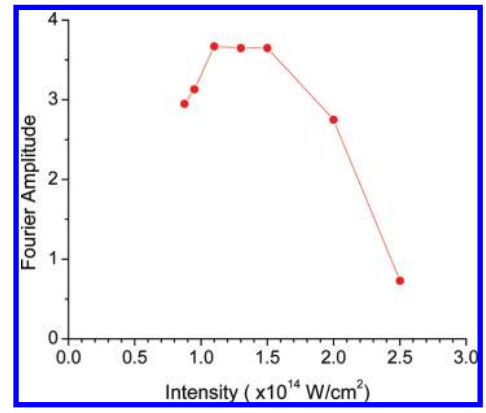

Figure 2. Fourier amplitude of the 5.18 eV peak for a Gaussian pulse envelope with fwhm = 3.5 fs, $\omega = 0.06$ au, and $\phi = 0$ for field intensities of 0.875, 0.95, 1.1, 1.3, 1.5, 2.0, and 2.5×10^{14} W/cm^2.

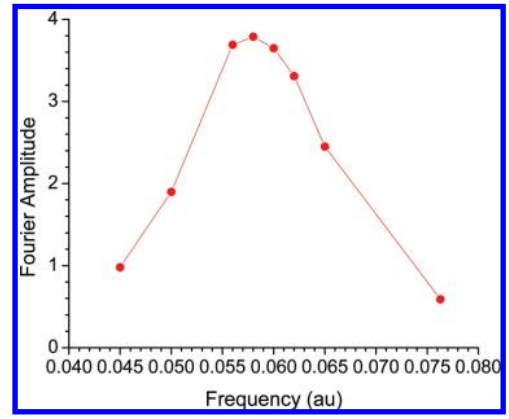

Figure 3. Fourier amplitude of the 5.18 eV peak for a Gaussian pulse envelope with fwhm = 3.5 fs, $\phi = 0$, intensity = 1.3×10^{14} W/cm^2 for frequencies of 0.045, 0.050, 0.056, 0.058, 0.060, 0.062, 0.065, and 0.753 au.

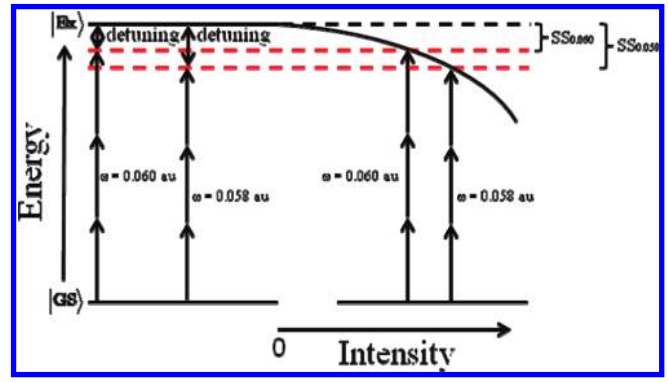

Figure 4. A representation of the Stark-shifting for the 5.18 eV state showing the resonances of photons of two energies and how this affects the intensity for each resonance.

eight frequencies while keeping the intensity, fwhm, and phase constant at $I = 1.3 \times 10^{14}$ W/cm^2, fwhm = 3.5 fs, and $\phi = 0$, respectively. Figure 3 shows a peak in the Fourier amplitude at a frequency of 0.058 au, suggesting a CO_2^+ resonance at 4.735 eV which is slightly different from the resonance energy suggested in Figure 2. To understand the phenomenon, we present an energy level model in Figure 4 that depicts the Stark-shifting of the 5.18 eV state into resonance with the photons of frequencies 0.06 and 0.058 au. The calculations for the data shown in Figure 2 employ a carrier frequency of 0.06 au to explore the intensity dependence of the 5.18 eV peak height. The resonant excitation maximum intensity was found to be 1.1×10^{14} W/cm^2. Figure 4 shows that the Stark-shifting ($SS_{0.060}$

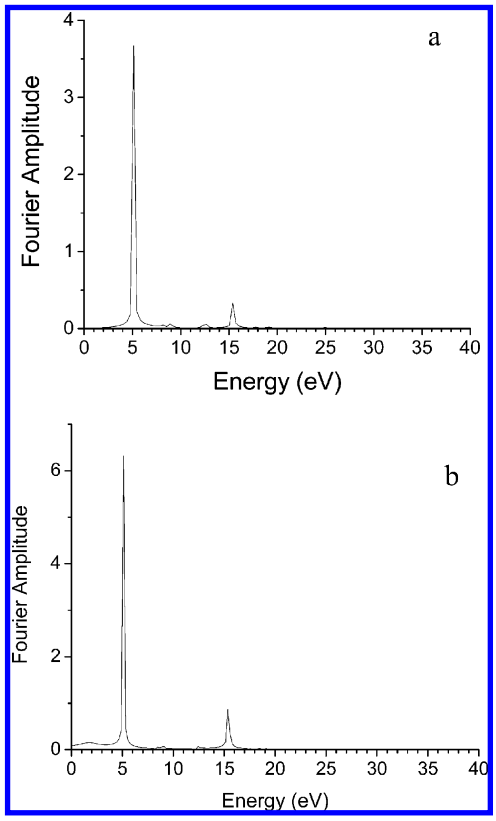

Figure 5. CO_2^+ excited state spectra for a Gaussian pulse envelope with $\omega = 0.06$ au, $\phi = 0$, and intensity $= 1.1 \times 10^{14}$ W/cm^2 with fwhm (a) 3.5 and (b) 5.6 fs.

in Figure 4) required is on the order of the detuning for the three-photon resonance. For excitation at a frequency of 0.06 au, this occurs at 1.1×10^{14} W/cm^2. At 1.3×10^{14} W/cm^2, the 5.18 eV state Stark-shifts into resonance with three-photon excitation at 0.058 au.

To explore the effect of the Stark-shift model, we increase the pulse duration from three to five cycles by increasing the fwhm. Increasing the fwhm of the pulse should make the response slightly more adiabatic because the ramping time to the maximum electric field increases, making the cycle-to-cycle changes in E_{max} smaller in comparison with a shorter pulse. This slower intensity ramp maintains the 5.18 eV state near resonance for a longer time, thereby increasing the excitation probability. This should result in a larger Fourier amplitude for the 5.18 eV state as compared to the shorter pulse duration. The excitation spectra for the short pulse with parameters $I = 1.1 \times 10^{14}$ W/cm^2, $\omega = 0.06$ au, and $\phi = 0$ and a pulse duration of 3 optical cycles is shown in Figure 5a, whereas the excitation spectra for the longer pulse of five optical cycles of the field with the same intensity, frequency, and phase as above is shown in Figure 5b. The Fourier amplitude of the 5.18 eV state for Figure 5a is 3.7; the Fourier amplitude for the longer pulse of Figure 5b increases 70% to 6.3, as anticipated. This suggests that the response of the Fourier amplitude for field intensities from ~0.875 to 2×10^{14} W/cm^2 is due to a three-photon resonance induced by the Stark-shifting of the 5.18 eV state.

The Stark shift of the 5.18 eV state under the conditions of Figure 3 (with optimal frequency of 0.058 au), is ~0.425 eV. Although an analytical estimation of the strong field Stark-shifting is not possible at this time, the strong field approach of reference 29 is promising.

(b) Nonadiabatic Excitation. Although resonant three-photon excitation seems to dominate the excitation process at low intensities, Figure 1b also suggests that nonadiabatic excitation dominates the excitation process at higher intensities from 2.5 to 5.0×10^{14} W/cm^2. This is seen in the exponential growth of the Fourier amplitudes for the four main peaks at 5.18, 9.0, 12.5, and 15.4 eV. The bound state electron dynamics described at these higher intensities where the 5.18 eV excited state is Stark-shifted through the three-photon resonance are consistent with NME theory. The calculations at these higher intensities also demonstrate an increase in excitation volume with increasing laser intensity, in agreement with the NME model.

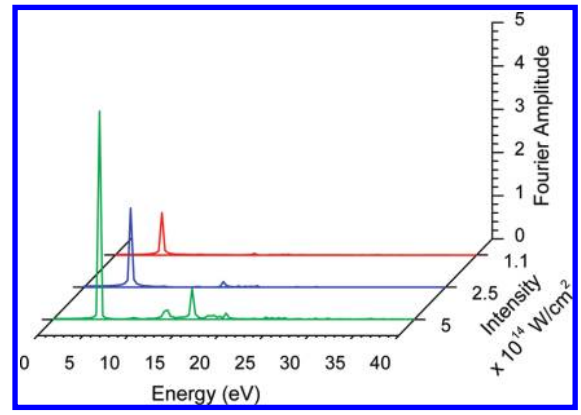

Figure 6. CO_2^+ excited state spectra for a Gaussian pulse envelope with $\omega = 0.045$ au, $\phi = 0$, and fwhm 3.5 fs for intensities of 1.3, 2.5, and 5.0×10^{14} W/cm^2.

To test the hypothesis that nonadiabatic excitation dominates the bound state electron dynamics at the higher intensities, we calculate bound state dynamics for an excitation frequency that is far from the near-three-photon resonance. The cation bound state electron dynamics were calculated using the following parameters: fwhm $= 3.5$ fs, $\omega = 0.045$ au, and $\phi = 0$ for intensities of 1.1, 2.5, and 5.0×10^{14} W/cm^2. Figure 6 shows the excitation spectrum under these conditions far from the three-photon resonance. The excitation spectrum shows a nonlinear increase in the excitation volume with increasing intensity, as expected for nonadiabatic excitation from NME theory. Note that the feature at the 5.18 eV peak also responds in the expected exponential manner. The response of the excitation volumes for the three highest intensities shown in Figure 1b (from 2.5 through 5.0×10^{14} W/cm^2) at a frequency of 0.06 au also respond exponentially. This suggests that nonadiabatic excitation is the dominant excitation process for these larger intensities where the 5.18 eV state has been Stark-shifted through the near-three-photon resonance.

To directly compare the TDHF simulations to NME theory, the integrated excitation volumes are compared to the integrated excitation probability in Figure 7 for excitation frequencies of 0.045 and 0.060 au. The normalized excitation probability, for a frequency of 0.045 au, is plotted as a function of electric field strength and is shown in Figure 7a, revealing qualitative agreement between TDHF and NME theory in the case when nonadiabatic excitation is the dominate excitation mechanism. Figure 7b displays the normalized excitation probability for a frequency of 0.06 au as a function of the electric field strength for both NME theory and TDHF at the larger intensities from 2.5 through 5.0×10^{14} W/cm^2. Figure 7b reveals that at the three highest intensities, NME theory and TDHF also qualitatively agree. There is some deviation in the nonadiabatic excitation probability between TDHF and NME theory in Figure 7b.

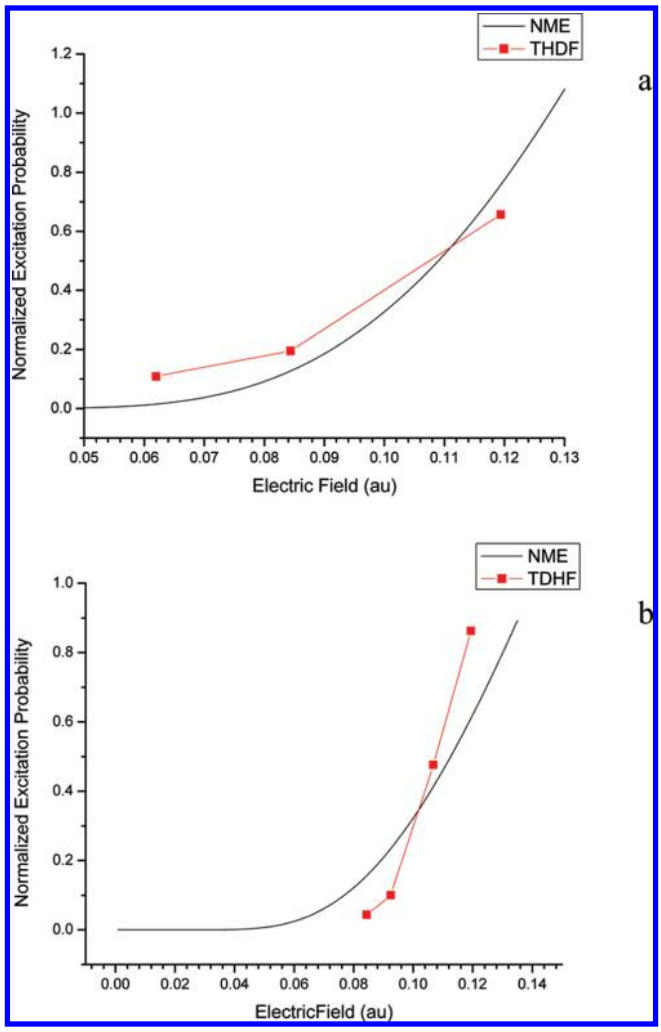

Figure 7. Normalized excitation probability using NME theory and TDHF for a Gaussian pulse shape with fwhm = 3.5 fs for frequencies (a) $\omega = 0.045$ au and (b) $\omega = 0.06$ au.

The excitation probability for TDHF rises more rapidly than the excitation probability using NME theory. This is due to two factors. The first factor arises from the fact that NME theory is derived from Landau−Dykhne theory. This assumes that the doorway state energy, Δ_0, does not get smaller; however, TDHF theory shows that Stark-shifting of this state to a lower energy can occur. The Stark shift decreases Δ_0 and thereby increases the NME excitation probability. The current version of NME theory does not include the possible decrease in energy of the Δ_0, and it will not quantitatively agree with TDHF theory. The second factor is due to the Stark-shifting of the Δ_0 state. The transition dipole, μ, may also change, thus affecting the excitation probability and the dynamic polarizabilty, α. Such extensions to NME theory, along with the extensions to the dynamic Stark-shifting of reference 29, will be described in a subsequent publication. The approach of reference 29 must be extended to include multiple electron effects though the addition of polarizabilty, and excitation for $\Delta l > 0$ must be allowed for accurate prediction of Stark-shifting in molecules, which will then be used to calculate the decrease in Δ_0. Additionally, it may be possible to use the theory of reference 29 or the Zakhorov-Shabat[46] equations to model both resonant and nonadiabatic excitation; however, both theories require extension to multiple electrons and multiple excited states to directly compare nonadiabatic excitation from NME theory.

We have determined that Figure 1b demonstrates the transition from resonant (for intensities from 0.875 to 2.0 × 10^{14} W/cm^2) to nonadiabatic excitation (for intensities 2.5 × 10^{14} W/cm^2 and larger) for three-cycle laser pulses at a frequency of 0.06 au. The characteristics of resonant excitation are an increase in the excitation volume and peak height of the resonant state with a slight increase in pulse duration (shown in Figure 5), and an increase and then decrease in peak height with an increase in electric field intensity (shown in Figure 1b), with very minor excitation in the nonresonant states (shown in Figures 1a, b and 5). Figures 1b and 6 display the characteristics of nonadiabatic excitation, consisting of an exponential increase in the excitation volume and the peak heights for all the excited states below the ionization potential. The peak height for each excited state does not follow the magnitude of the transition dipole from the ground to excited states. The ground-to-excited state transition dipole magnitudes of the main four excited states in decreasing order are 1.3, 0.81, 0.39, and 0.25 au for the 15.44, 5.18, 12.49, and 9.03 eV states, respectively (see Table 1), whereas excited state peak heights follow the order 5.18 > 15.44 > 12.49 > 9.03 eV. Furthermore, the order of the excitation process for the three states with the largest peak heights can be obtained from the slope of a plot of the log of the excitation volume versus the log of the laser intensity. Analysis reveals orders of 4.39, 5.13, and 4.64 for the 5.18, 12.49, and 15.44 eV states, respectively. These slopes (orders) suggest that multiphoton excitation is not the dominant mechanism, since we would have expected orders of 3, 7, and 10, respectively, for this mechanism. Thus, we propose that the nonadiabtic excitation is governed by the interplay between the excited state energy and the transition dipole moments between the ground and excited states.

Summary

We have studied the bound state electron dynamics induced by strong-field ultrashort laser pulses (on the order of three optical cycles of the field) in a linear triatomic molecular monocation CO_2^+ as a function of pulse intensity and carrier frequency. In this regime, the transition from a near-resonant to nonadiabatic excitation mechanism was observed. Fourier analysis of the residual dipole moment oscillations as a function of intensity revealed excitation spectra that showed either near-resonant nonlinear excitation or nonadiabatic excitation. Following the change under a systematic increase in intensity from 0.875 to 2.0 × 10^{14} W/cm^2 revealed resonant excitation due to the Stark-shifting of the 5.18 eV state. This Stark-shifting was 0.425 eV for an intensity of 1.3 × 10^{14} W/cm^2. Nonadiabatic excitation was the dominant mechanism at intensities >2.0 × 10^{14} W/cm^2. The near-resonant excitation caused an increase and then a decrease in the Fourier amplitude of the 5.18 eV state with increasing electric field intensity. At this Stark-shifted resonance, the excitation volume of the 5.18 eV state was the largest, and the excitation volumes of all other excited states was minimal. The characteristic of nonadiabatic excitation was an exponential increase in the excitation volume of all four lowest-energy excited states. Thus, the difference between adiabatic and nonadiabatic excitation was readily discernible.

Acknowledgment. S.S. and D.R. acknowledge very useful conversations with A. Stolow, O. Smirnova, M. Ivanov, and Xiaosong Li and funding from the National Science Foundation, Grant nos. CHE0518497 to R.J.L. and CHE0512144 to H.B.S.

References and Notes

(1) Dudovich, N.; Polack, T.; Pe′er, A.; Silberberg, Y. Simple Route to Strong-Field Coherent Control. *Phys. Rev. Lett.* **2005**, *94*, 083002.

(2) Levis, R. J.; Menkir, G. M.; Rabitz, H. Selective Bond Dissociation and Rearrangement with Optimally Tailored, Strong-Field Laser Pulses. *Science* **2001**, *292*, 709.

(3) Wollenhaupt, M.; Liese, D.; Prakelt, A.; Sarpe-Tudoran, C.; Baumert, T. Quantum Control by Ultrafast Dressed States Tailoring. *Chem. Phys. Lett.* **2006**, *419*, 184.

(4) Wollenhaupt, M.; Prakelt, A.; Sarpe-Tudoran, C.; Liese, D.; Baumert, T. Quantum Control by Selective Population of Dressed States Using Intense Chirped Femtosecond Laser Pulses. *Appl. Phys. B: Lasers Opt.* **2006**, *82*, 183.

(5) Wells, E.; Krishnamurthi, V.; Carnes, K. D.; Johnson, N. G.; Baxter, H. D.; Moore, D.; Bloom, K. M.; Barnes, B. M.; Tawara, H.; Ben-Itzhak, I. Proton-Carbon Monoxide Collisions from 10 KeV to 14 MeV. *Phys. Rev. A* **2005**, *72*, 022726.

(6) Sola, I. R.; Chang, B. Y.; Rabitz, H. Manipulating Bond Lengths Adiabatically with Light. *J. Chem. Phys.* **2003**, *119*, 10653.

(7) Sussman, B. J.; Townsend, D.; Ivanov, M. Y.; Stolow, A. Dynamic Stark Control of Photochemical Processes. *Science* **2006**, *314*, 278.

(8) Sussman, B. J.; Underwood, J. G.; Lausten, R.; Ivanov, M. Y.; Stolow, A. Quantum Control Via the Dynamic Stark Effect: Application to Switched Rotational Wave Packets and Molecular Axis Alignment. *Phys. Rev. A* **2006**, *73*, 053403.

(9) Sussman, B. J.; Ivanov, M. Y.; Stolow, A. Nonperturbative Quantum Control Via the Nonresonant Dynamic Stark Effect. *Phys. Rev. A* **2005**, *71*, 051401.

(10) Gibson, G. N. Adiabatic Passage on High-Order Multiphoton Transitions. *Phys. Rev. A* **2005**, *72*, 041404.

(11) Bartels, R. A.; Weinacht, T. C.; Leone, S. R.; Kapteyn, H. C.; Murnane, M. M. Nonresonant Control of Multimode Molecular Wave Packets at Room Temperature. *Phys. Rev. Lett.* **2002**, *88*, 033001.

(12) Lezius, M.; Blanchet, V.; Ivanov, M. Y.; Stolow, A. Polyatomic Molecules in Strong Laser Fields: Nonadiabatic Multielectron Dynamics. *J. Chem. Phys.* **2002**, *117*, 1575.

(13) Lezius, M.; Blanchet, V.; Rayner, D. M.; Villeneuve, D. M.; Stolow, A.; Ivanov, M. Y. Nonadiabatic Multielectron Dynamics in Strong Field Molecular Ionization. *Phys. Rev. Lett.* **2001**, *86*, 51.

(14) Markevitch, A. N.; Romanov, D. A.; Smith, S. M.; Schlegel, H. B.; Ivanov, M. Y.; Levis, R. J. Sequential Nonadiabatic Excitation of Large Molecules and Ions Driven by Strong Laser Fields. *Phys. Rev. A* **2004**, *69*, 013401.

(15) Markevitch, A. N.; Smith, S. M.; Romanov, D. A.; Schlegel, H. B.; Ivanov, M. Y.; Levis, R. J. Nonadiabatic Dynamics of Polyatomic Molecules and Ions in Strong Laser Fields. *Phys. Rev. A* **2003**, *68*, 011402.

(16) Dewitt, M. J.; Levis, R. J. Near-Infrared Femtosecond Photoionization Dissociation of Cyclic Aromatic Hydrocarbons. *J. Chem. Phys.* **1995**, *102*, 8670.

(17) DeWitt, M. J.; Levis, R. J. Observing the Transition from a Multiphoton-Dominated to a Field-Mediated Ionization Process for Polyatomic Molecules in Intense Laser Fields. *Phys. Rev. Lett.* **1998**, *81*, 5101.

(18) DeWitt, M. J.; Peters, D. W.; Levis, R. J. Photoionization/Dissociation of Alkyl Substituted Benzene Molecules Using Intense Near-Infrared Radiation. *Chem. Phys.* **1997**, *218*, 211.

(19) Campbell, E. E. B.; Hoffmann, K.; Rottke, H.; Hertel, I. V. Sequential Ionization of C-60 with Femtosecond Laser Pulses. *J. Chem. Phys.* **2001**, *114*, 1716.

(20) Kosmidis, C.; Tzallas, P.; Ledingham, K. W. D.; McCanny, T.; Singhal, R. P.; Taday, P. F.; Langley, A. J. Multiply Charged Intact Ions of Polyatomic Cyclic Molecules Generated by a Strong Laser Field. *J. Phys. Chem. A* **1999**, *103*, 6950.

(21) Talebpour, A.; Larochelle, S.; Chin, S. L. Multiphoton Ionization of Unsaturated Hydrocarbons. *J. Phys. B* **1998**, *31*, 2769.

(22) Frasinski, L. J.; Codling, K.; Hatherly, P.; Barr, J.; Ross, I. N.; Toner, W. T. Femtosecond Dynamics of Multielectron Dissociative Ionization by Use of Picosecond Laser. *Phys. Rev. Lett.* **1987**, *58*, 2424.

(23) Frasinski, L. J.; Codling, K.; Hatherly, P. A. Covariance Mapping—a Correlation Method Applied to Multiphoton Multiple Ionization. *Science* **1989**, *246*, 1029.

(24) Boyle, M.; Hoffmann, K.; Schulz, C. P.; Hertel, I. V.; Levine, R. D.; Campbell, E. E. B. Excitation of Rydberg Series in C-60. *Phys. Rev. Lett.* **2001**, *87*, 273401.

(25) Anderson, N. A.; Durfee, C. G.; Murnane, M. M.; Kapteyn, H. C.; Sension, R. J. The Internal Conversions of Trans- and *cis*-1,3,5-Hexatriene in Cyclohexane Solution Studied with Sub-50 fs UV Pulses. *Chem. Phys. Lett.* **2000**, *323*, 365.

(26) Anderson, N. A.; Pullen, S. H.; Walker, L. A.; Shiang, J. J.; Sension, R. J. Ultrafast Polyene Dynamics in Solution: The Conformational Relaxation and Thermalization of Highly Excited *cis*-1,3,5-Hexatriene as a Function of Initial Conformation and Solvent. *J. Phys. Chem. A* **1998**, *102*, 10588.

(27) DeWitt, M. J.; Levis, R. J. Calculating the Keldysh Adiabaticity Parameter for Atomic, Diatomic, and Polyatomic Molecules. *J. Chem. Phys.* **1998**, *108*, 7739.

(28) Markevitch, A. N.; Moore, N. P.; Levis, R. J. The Influence of Molecular Structure on Strong Field Energy Coupling and Partitioning. *Chem. Phys.* **2001**, *267*, 131.

(29) Trallero-Herrero, C.; Cardoza, D.; Weinacht, T. C.; Cohen, J. L. Coherent Control of Strong Field Multiphoton Absorption in the Presence of Dynamic Stark Shifts. *Phys. Rev. A* **2005**, *71*, 013423.

(30) Trallero-Herrero, C.; Cohen, J. L.; Weinacht, T. Strong-Field Atomic Phase Matching. *Phys. Rev. Lett.* **2006**, *96*, 063603.

(31) Freeman, R. R.; Bucksbaum, P. H.; Milchberg, H.; Darack, S.; Schumacher, D.; Geusic, M. E. Above-Threshold Ionization with Subpicosecond Laser Pulses. *Phys. Rev. Lett.* **1987**, *59*, 1092.

(32) Posthumus, J. H. The Dynamics of Small Molecules in Intense Laser Fields. *Rep. Prog. Phys.* **2004**, *67*, 623.

(33) Bandrauk, A. D.; Ruel, J. Charge-Resonance-Enhanced Ionization of Molecular Ions in Intense Laser Pulses: Geometric and Orientation Effects. *Phys. Rev. A* **1999**, *59*, 2153.

(34) Li, X. S.; Smith, S. M.; Markevitch, A. N.; Romanov, D. A.; Levis, R. J.; Schlegel, H. B. A Time-Dependent Hartree-Fock Approach for Studying the Electronic Optical Response of Molecules in Intense Fields. *Phys. Chem. Chem. Phys.* **2005**, *7*, 233.

(35) Frisch, M. J.; Trucks, G. W.; Schlegel, H. B.; Scuseria, G. E.; Robb, M. A.; Cheeseman, J. R.; Montgomery, J. A., Jr.; Vreven, T.; Kudin, K. N.; Burant, J. C.; Millam, J. M.; Iyengar, S. S.; Tomasi, J.; Barone, V.; Mennucci, B.; Cossi, M.; Scalmani, G.; Rega, N.; Petersson, G. A.; Nakatsuji, H.; Hada, M.; Ehara, M.; Toyota, K.; Fukuda, R.; Hasegawa, J.; Ishida, M.; Nakajima, T.; Honda, Y.; Kitao, O.; Nakai, H.; Klene, M.; Li, X.; Knox, J. E.; Hratchian, H. P.; Cross, J. B.; Bakken, V.; Adamo, C.; Jaramillo, J.; Gomperts, R.; Stratmann, R. E.; Yazyev, O.; Austin, A. J.; Cammi, R.; Pomelli, C.; Ochterski, J. W.; Ayala, P. Y.; Morokuma, K.; Voth, G. A.; Salvador, P.; Dannenberg, J. J.; Zakrzewski, V. G.; Dapprich, S.; Daniels, A. D.; Strain, M. C.; Farkas, O.; Malick, D. K.; Rabuck, A. D.; Raghavachari, K.; Foresman, J. B.; Ortiz, J. V.; Cui, Q.; Baboul, A. G.; Clifford, S.; Cioslowski, J.; Stefanov, B. B.; Liu, G.; Liashenko, A.; Piskorz, P.; Komaromi, I.; Martin, R. L.; Fox, D. J.; Keith, T.; Al-Laham, M. A.; Peng, C. Y.; Nanayakkara, A.; Challacombe, M.; Gill, P. M. W.; Johnson, B.; Chen, W.; Wong, M. W.; Gonzalez, C.; Pople, J. A. *Gaussian*, version d01+; Gaussian, Inc.: Wallingford CT, 2006.

(36) Kendall, R.; Dunning, T. H.; Harrison, R. J. *J. Chem. Phys.* **1992**, *96*, 6796.

(37) Woon, D. E.; Dunning, T. H. *J. Chem. Phys.* **1993**, *98*, 1358.

(38) Winter, N. W.; Bender, C. F.; Goddard, W. A. Theoretical Assignments of Low-Lying Electronic States of Carbon Dioxide. *J. Chem. Phys.* **1973**, *20*, 480.

(39) Corkum, P. B. Plasma Perspective on Strong-Field Multiphoton Ionization. *Phys. Rev. Lett.* **1993**, *71*, 1994.

(40) Smith, S. M.; Li, X. S.; Markevitch, A.; Romanov, D.; Levis, R. J.; Schlegel, H. B. Numerical Simulation of Nonadiabatic Electron Excitation in the Strong-Field Regime. 3. Polyacene Neutrals and Cations. *J. Phys. Chem. A* **2007**, *111*, 6920.

(41) Smith, S. M.; Li, X. S.; Markevitch, A. N.; Romanov, D. A.; Levis, R. J.; Schlegel, H. B. Numerical Simulation of Nonadiabatic Electron Excitation in the Strong Field Regime. 2. Linear Polyene Cations. *J. Phys. Chem. A* **2005**, *109*, 10527.

(42) Barth, C. A.; Fastie, W. G.; Hord, C. W.; Pearce, J. B.; Kelly, K. K.; Stewart, A. I.; Thomas, G. E.; Anderson, G. P.; Raper, O. F. Mariner-6—Untraviolet Spectrum of Mars Upper Atmosphere. *Science* **1969**, *165*, 1004.

(43) Rostas, J.; Tuckett, R. P. The Emission-Spectrum of $CO_2^{(+)}$ —the B2-Sigma-U+ (000)-] X2-Pi-G (000) Band, Rotationally Cooled in a Molecular-Beam. *J. Mol. Spectrosc.* **1982**, *96*, 77.

(44) Brommer, M.; Chambaud, G.; Reinsch, E. A.; Rosmus, P.; Spielfiedel, A.; Feautrier, N.; Werner, H. J. Theoretical Potential-Energy Function and Rovibronic Spectrum of CO^{2+} (X2-Pi-G). *J. Chem. Phys.* **1991**, *94*, 8070.

(45) Leonard, C.; Diehr, M.; Rosmus, P.; Maguire, W. C. Radiative Transition Probabilities in the X-2 Pi(G) State of CO^{2+}. *J. Quant. Spectrosc. Radiat. Transfer* **2008**, *109*, 535.

(46) McCann, J. F.; Bandrauk, A. D. Eigenvalues of the Zakharov—Shabat Equations by Semiclassical Approximation. *Phys. Lett. A* **1990**, *151*, 509.

JP907372K